ECLÉTICA QUÍMICA

Eclet. Quim. 51 | e-1604, 2026

Original Articles in Chemistry and Related Areas

https://doi.org/10.26850/1678-4618.eq.v51.2026.e1604

Physical cross-linking of starch hydrogel by short cycles of cooling and heating in the presence of glycerol for potential use as dermal dressing

Mariana **Fornaizer**[1+], Harumi **Otaguro**[2]

Abstract

This study focused on developing films from physically cross-linked starch hydrogel with glycerol, utilizing short cooling and heating cycles to enhance cross-linking via the freeze-thaw process. Characterization revealed that 30% glycerol promoted physical cross-linking, further intensified by the thermal cycles, leading to increased film density (AG-R1, AG-R2, and AG-R4). The films demonstrated favorable physicochemical properties for reparative dressings, including easy handling, flexibility, high swelling capacity, water vapor permeability, and low solubility. Notably, the AG-R2 film exhibited the most significant changes, showing increased density and reduced thickness. This indicates a distinct morphology compared to the other films, suggesting an entanglement that restricts solvent molecules (water) incorporation during testing.

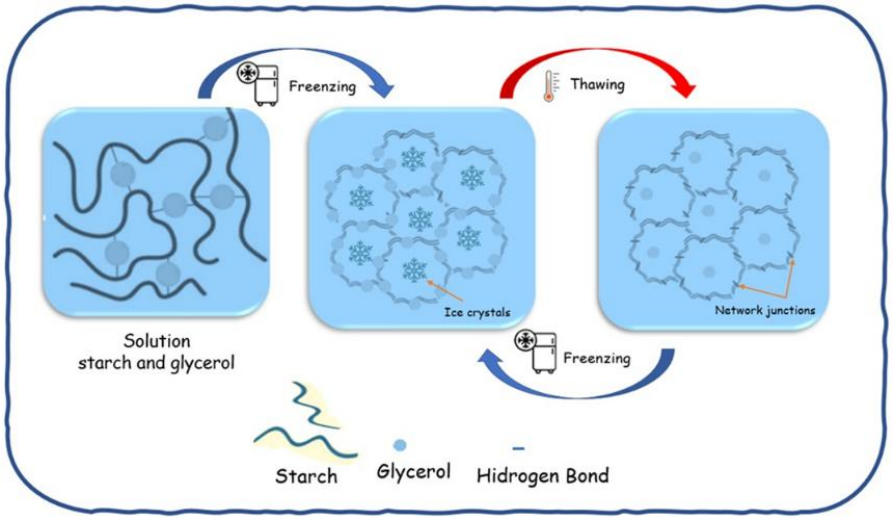

Article History

Received November 02, 2024
Accepted May 08, 2025
Published May 12, 2026

Keywords

1. hydrogel biomaterials;
2. dermal applications;
3. biodegradable polymers;
4. thermal processing;
5. wound healing.

Section Editors

Rogéria Rocha **Gonçalves**

Highlights

- Starch hydrogel films exhibit improved properties with glycerol addition.
- Short cooling and heating cycles enhance physical cross-linking effects.
- AG-R2 film shows unique morphology, increasing density and reducing thickness.

[1]Federal University of Uberlândia, Institute of Chemistry, Uberlândia, Brazil. [2]Federal University of Paraná, Center for Marine Studies, Pontal do Paraná, Brazil. **+Corresponding author:** Mariana Fornaizer, **Phone:** +34991178266, **Email address** mariana-for@hotmail.com

1. Introduction

The growth of studies related to the regenerative medicine area, aiming at the development of new biomaterials that interact and induce the formation of new tissues, restoring, maintaining or even improving tissue function, is growing every day (Mantha *et al.*, 2019; Zeng *et al.*, 2022). In this way, the investment in the development of technologies in biomaterials (Long *et al.*, 2022), which allow the repair of compromised tissues, either by healing or regeneration, appears to be very promising (Fan *et al.*, 2022; Long *et al.*, 2022).

Research in the field of biomaterials and their medical applications indicate that natural polymer hydrogels in the form of films, such as systems based on polysaccharides such as starch (Palanisamy *et al.*, 2022; Rodrigues *et al.*, 2021), represent promising alternatives for the production of biomedical materials, due to their biocompatibility, atoxicity and bioabsorption even in internal use (Palanisamy *et al.*, 2022; Rodrigues *et al.*, 2021; Savencu *et al.*, 2021). However, its application demands changes, aiming to provide better mechanical properties and mainly reduce its solubility (Pires and Moura, 2017; Rodrigues *et al.*, 2021; Souza *et al.*, 2022).

In this sense, regarding the improvement of mechanical properties, this can be achieved by incorporating a plasticizing agent, such as glycerol (Ben *et al.*, 2022), which promotes the reduction of intermolecular interactions between starch chains adjacent, resulting in increased mobility of these chains and, consequently in obtaining flexible materials (Wang *et al.*, 2022). The use of these components together (starch and glycerol), as described in the study by Rodrigues *et al.* (2021) provides a reduction in the solubility of starch films, when incorporated in concentrations above 30% in relation to the mass of starch, due to the formation of cross-linking bonds of glycerol with starch chains via the physical cross-linking process.

The crosslink process is an alternative for modifying the characteristics of starch films, mainly in relation to the reduction of their solubility (He *et al.*, 2022; Jia *et al.*, 2023). Cross-linking is a type of chemical or physical modification, which aims to unite polymer chains (Jia *et al.*, 2023). In the chemical crosslink method, chains are covalently joined through the use of reticulating agents. In the physical crosslink method, the chains are joined by non-covalent interactions, dispensing with the use of a reticulating agent (Jia *et al.*, 2023; Yan *et al.*, 2023).

There has been increasing interest in physical or reversible gels due to the relative ease of production and the advantage of not using cross-linking agents (Rodrigues *et al.*, 2021; Dong *et al.*, 2022). The achievement by the physical cross-linking process depends on two main criteria: the interaction between the chain must be strong enough to form a semi-permanent junction in the molecular network and the network must contain a large amount of water molecules within it (Bai *et al.*, 2022; Dong *et al.*, 2022). The forces involved in the formation of the physical gel are hydrophobic, electrostatic and hydrogen bonds between polymeric chains (Bai *et al.*, 2022).

With this, the elaboration of films from the physically crosslinked starch hydrogel proves to be a promising alternative for use as dermal dressings (Lu *et al.*, 2022). However, knowing that hydrogels crosslinked only by hydrogen bonding have some disadvantages, such as difficult injection and poor mechanical strength due to their high content and low cross-linking density (Bai *et al.*, 2022; Lu *et al.*, 2022), Guo *et al.*, (2022) highlight the possibility of combining hydrogen bonding with other types of physical cross-linking techniques, such as the freezing-thawing process.

In the freezing-thawing process, cryogels are formed from the freezing of homogeneous polymeric solutions, their storage in the glassy state and subsequent thawing (Gerrits *et al.*, 2024; Guo *et al.*, 2022). In said process, the gelation of the polymer by the freezing and thawing mechanism is conducted by the phase separation that occurs when the solution freezes and the polymer is rejected from the growing ice crystals, a process that is optimized with repeated cycles (Abdullah *et al.*, 2022). Physical freeze-thawing cross-linking is possible due to the existence of regular pendant hydroxyl groups in starch that can form crystallites by strong hydrogen bonding between chains (Xiang *et al.*, 2022).

Considering that most of the studies that make use of the cross-linking process via freezing-thawing take days to carry out the physical cross-linking (Abdullah *et al.*, 2022; Gerrits *et al.*, 2024; Guo *et al.*, 2022), the study in question seeks to promote adaptations in this process, making use of short cycles of cooling and heating, instead of the traditional freezing-thawing process. In this sense, the study proposes using short cooling and heating cycles to favor physical cross-linking in the polymeric matrix, which is based on the principle of physical cross-linking via freezing-thawing.

Thus, this work studied the development of films from physically crosslinked starch hydrogel in the presence of glycerol via short cooling and heating cycles. The study focuses on developing a film with potential use as dressings based on a physical cross-linking process via short cooling and heating cycles.

2. Experimental

2.1. Reagents and solutions

Cassava starch (Manihot utilissima) refers to the starch product extracted from the ground and edible parts of the plant. It contains approximately 25% amylose and 75% amylopectin. The starch was commercially acquired locally, and glycerol was obtained from Neon®. Phosphate buffered saline (PBS) was prepared by mixing sodium hydroxide (Vetec), sodium dihydrogen phosphate (Carlo ErbaReagents), and deionized water.

2.2. Physical cross-linking of starch hydrogel by cooling and heating cycles

From the same concentration of cassava starch (5% m/v of water) glycerol was incorporated at a concentration of 30% (m/m) in relation to the mass of starch. For each formulation, the starch and glycerol were diluted in 75.00 mL of deionized water and heated in a microwave oven at 30 W for 2 min for gelatinization to occur (75 °C). Then, more solvent (75.00 mL) was added, and the systems were mechanically stirred for 20 min. The hydrogels were then subjected to the physical cross-linking process by cooling and heating cycles for 20 min each, and they were stored in a conventional freezer at 0 °C and a thermostated bath at 40 °C, respectively. The hydrogels were developed with different cycles.

2.2.1. Elaboration of the films after the physical cross-linking process

After the hydrogel cross-linking process, the different starch films were developed using the casting method (Fornazier *et al.*, 2021). The remaining solvent (100.00 mL of water) was added to the hydrogels, obtaining filmogenic solutions. These solutions were poured into plastic molds and allowed to dry in an oven at 35 °C for 48 h. At the end of the drying time, the resulting films were removed and stored.

2.3. Characterization of films

2.3.1. Determination of thickness, density and grammage

The films were cut into 6.0 cm^2, then dried in an oven at 40 °C for 2 h and weighed on analytical balance. Subsequently, the thickness (e) was determined at 4 different points using a ZAAS digital micrometer. A calibrated pycnometer measured the density of films, and distilled water was used as the immersing liquid. A 10.00 mL pycnometer with known mass was used to calculate the pycnometer mass with water, water density and the pycnometer mass with water and starch film.

The added water volume was obtained from the water density value at the working temperature (d = 0.9962 g cm^{-3}). The density was calculated by **Eq. 1**, where m is the mass of the film (g), V_p is the pycnometer volume (mL), and V_a is the volume of water (mL).

$$d = \frac{m}{V_{p-Va}} \quad (1)$$

The grammage was calculated by **Eq. 2**, where m is the film mass (g) and A is the sample area.

$$\text{Grammage} = \frac{m}{A} \quad (2)$$

2.3.2. Water vapor permeability

The water vapor permeability of the film was studied using the cup of Payne method. The film was first cut into a circular shape larger than the cup's inner diameter. Then, the cup was placed on a horizontal platform, and deionized water was placed inside the cup. Subsequently, the films were placed on top of the permeability cup. The cup was then covered and weighed to calculate the initial weight. The cup was then located inside a desiccator, using phosphorus pentoxide to generate a 20% relative humidity environment as a desiccant agent.

The cup weight was recorded at specified time intervals. The water vapor permeability (P_w) and water vapor transmission rate (J) were determined using **Eqs. 3** and **4**, where $\Delta m/\Delta t$ is the moisture gain weight per time (g/h), A is the exposed surface area of the film (cm^2), L is the thickness of the film (cm), and ΔP_v is the difference of partial pressure.

$$\frac{\Delta m}{\Delta t} x \frac{1}{A} = J \quad (3)$$

$$J = Pw\ x\ \frac{\Delta Pv}{L} \quad (4)$$

2.3.3. Scanning electron microscopy (SEM)

The morphology of the films was analyzed in relation to their surface and transversal section using the CARL ZEISS microscope MOD EVO MA10, with an acceleration voltage of 5 kV. Before analysis, the samples were coated with an ultrathin gold layer in a sputter coating system.

2.3.4. X-ray diffraction

X-ray diffraction analysis was performed on a Shimadzu XRD6000 apparatus (Shimadzu, Japan), operating at 40 kV with 3 mA of current and Cu Kα radiation (1.5406 A). The 2θ scan data were collected from 10° to 35° at a scanning speed of 1.0° min^{-1}.

2.3.5. Mechanical properties

The mechanical properties (i.e., tensile strength, Young's modulus, and elongation at break) of all the films were evaluated by uniaxial tensile testing using a universal Instron mechanical test machine model 5.982 with a 5.0 kN load cell. The films were cut into strips 0.75 cm wide by 4.0 cm long (ASTM D882-02, 2002), fixed in the apparatus, and subjected to a stress and strain test with a velocity of 25.0 mm min-1 and a distance between the claws of 2.0 cm.

The sample thickness was determined at five different points, using a ZAAS digital micrometer. Mechanical parameters were obtained from the stress-strain measures of each sample and expressed in MPa.

2.3.6. Swelling and solubility studies at physiological pH

The swelling and solubility studies were carried out under conditions close to the post-surgical environment, obtained using a phosphate-buffered saline solution (PBS), whose pH = 7.4 is close to the blood's physiological pH (pH = 7.35).

The swelling was evaluated in PBS medium using gravimetric (Fornazier *et al.*, 2021). The films were weighed (w_i) and then immersed in 10 mL PBS at 36.5 °C. At different periods, the samples were removed from the PBS, gently wiped with filter paper to remove the surface liquid and immediately weighed (w_f). The dilation ratio of the films was calculated using **Eq. 5**:

$$Swelling\ ratio = \frac{w_f - w_i}{w_i} \times 100 \quad (5)$$

For solubility studies, dry film samples were weighed (w_i), then immersed in PBS and incubated in a bath at 36.5 °C for 48 h. After the time interval samples were dried before weighing (w_f). The solubility was calculated by using the **Eq. 6**:

$$Solubility\ (\%) = \frac{w_i - w_f}{w_i} \times 100 \quad (6)$$

3. Results and discussion

3.1. Thickness, density and grammage

Biodegradables starch films were produced by the casting method, resulting in translucent, homogeneous, depigmented samples with very few lumps or bubbles (**Fig. 1**). Regarding the flexibility of the films, the samples with glycerol showed flexibility, allowing their handling without difficulty, while the pure film (A) was rigid, without flexibility. The flexibility of the AG-R1, AG-R2 and AG-R4 samples was not influenced by the cooling and heating cycles, presenting similar flexibility to the starch film containing glycerol (AG).

The addition of plasticizer, according to Rodrigues *et al.* (2021), leads to the formation of a morphology composed of free chains with fewer entanglements between them, making starch films more flexible. Thus, adding plasticizer improves the brittleness of the film, specifically the pure one, caused by high intermolecular forces.

https://doi.org/10.26850/1678-4618.eq.v51.2026.e1604

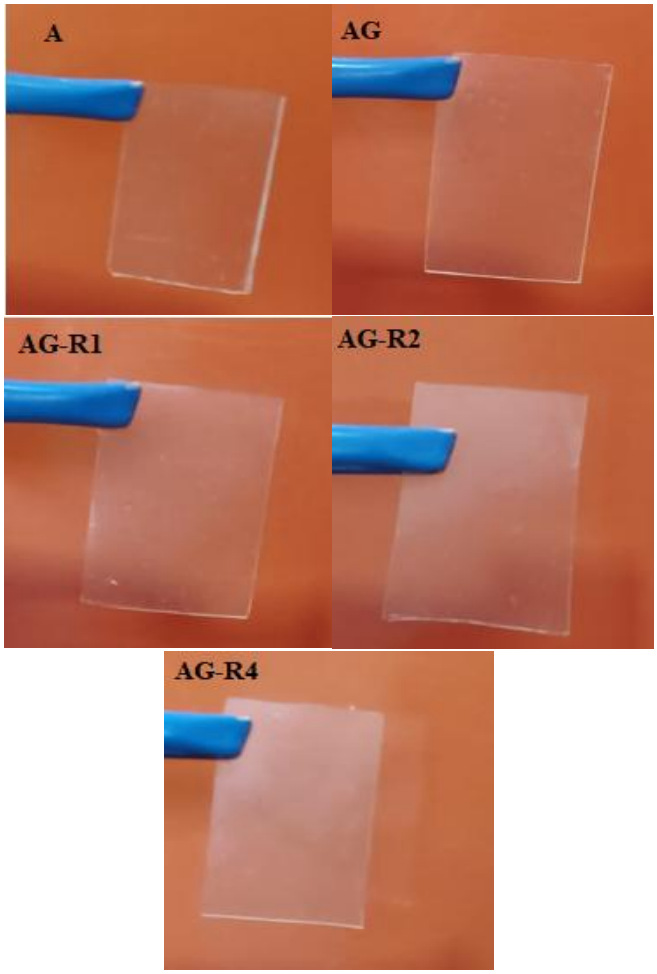

Figure 1. Photographs of the films produced **(A)** pure starch, **(AG)** starch with glycerol, **(AG-R1)** film submitted to a cooling/heating cycle, **(AG-R2)** two cycles and **(AG-R4)** four cycles.
Source: Elaborated by the authors.

The produced films exhibited varying thicknesses depending on their processing conditions (**Fig. 2**). Compared to standard film (A), adding glycerol resulted in an increase in thickness. According to Matta Jr. *et al.* (2011) in their discussion on starch and glycerol films, as filmogenic solutions dry and water evaporate, the solid content in the forming network becomes concentrated, which increases with the incorporation of glycerol. Thus, the increase in thickness due to the incorporation of glycerol is attributed to its action in interrupting the formation of the double helix of amylose with fragments of amylopectin, reducing the interaction between these molecules. The reduction in direct associations reduces gel retraction and increases the thickness of the films.

However, despite the equal amount of glycerol in all films, its effect on the thickness varied depending on the cooling-heating (cross-linking) process employed. In the case of the film cross-linked solely via hydrogen bonds (AG), the presence of glycerol resulted in a minimal increase in thickness. For films cross-linked in association with cooling and heating cycles, the variation in thickness was more pronounced for the AG-R1 film, while for the AG-R4 film, it remained nearly the same as that of the AG film. As for the AG-R2 film, there was a drastic reduction in thickness, even lower than that of the standard film. This fact demonstrates that, for this film, there was a greater interaction between the starch matrix and glycerol, that is, glycerol more easily penetrated the three-dimensional space of the starch, producing thinner films.

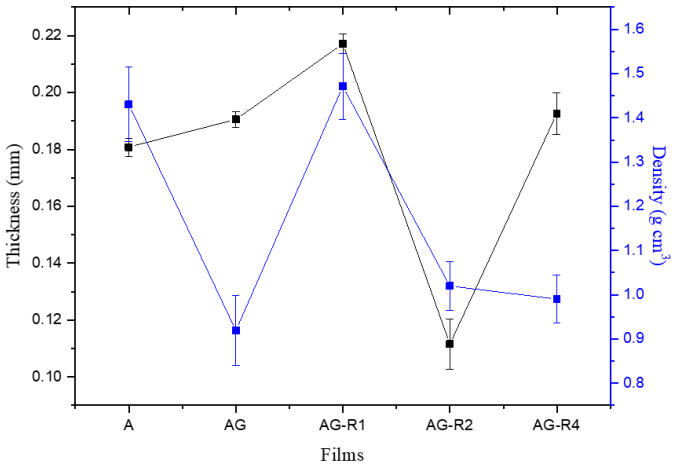

Figure 2. Relationship between thickness and density of starch films.
Source: Elaborated by the authors.

Regarding the density data (**Fig. 2**), an inverse behavior to the thickness data is observed. With the incorporation of glycerol (AG), an increase in thickness and a reduction in density are noted. This result is consistent, as an increase in thickness leads to an increase in volume and consequently a decrease in density, given that density is the ratio of the mass of material to the volume it occupies. These findings are like those of the study by Rodrigues *et al.* (2021), which incorporated different concentrations of glycerol in starch films.

Regarding films cross-linked via short cycles of cooling and heating, it is observed that the density increases upon conducting one cycle (AG-R1), approaching that of the pure starch film (A). However, upon increasing the cycles (AG-R2 and AG-R4), the density decreases again, approaching that of the AG film. The results indicate that increasing the cycles leads to a densification between the polymer chains (reduced volume), that is, a closer proximity between the chains, suggesting an effective physical cross-linking process via hydrogen bonds, thereby reducing the free volume between the chains.

When analyzing the films individually, it is observed that for the AG-R1 and AG-R4 films, an increase in thickness results in a reduction in density compared to pure starch, while for the AG-R2 film, there is a reduction in thickness compared to the others and an increase in density. These results indicate that short cycles of cooling and heating induce changes in the volume of the films, with this effect being more significant for the AG-R2 film.

This film showed an increase in density and a reduction in thickness, suggesting that the formed morphology is different from the other films, implying an entanglement that does not allow the incorporation of solvent molecules (water) used in the assay.

In the case of this film, it is evident that the cross-linking process within the matrix combined with the two short cycles of cooling and heating led to a more effective reduction in the film volume, indicating a higher efficiency in the cross-linking process formation. The significant densification resulted in a reduction in film thickness, due to the promotion of interactions between the molecules of the polymeric matrix.

Regarding the weight per unit area values of the films (**Table 1**), these are consistent with thickness data, as is calculated based on the weight and area of the film. The incorporation of glycerol into the films led to an increase in the solid content in the film composition, resulting in an increase in weight per unit area, as similarly observed by Costa *et al.* (2017). However, it is noted

that the AG-R2 film does not follow this pattern, like what occurred in the thickness and density data.

This profile strongly indicates that the adopted cross-linking method in its production resulted in a higher number of cross-links between the starch and glycerol chains in the film, reducing the distances between them and thus reducing its weight per unit area. This reduction is in line with the density and thickness data, indicating that the AG-R2 film has a smaller free volume when compared to the other films.

Table 1. Grammage of the films.

Films	Grammage (g cm^{-2})
A	0.024 ± 0.002
AG	0.029 ± 0.005
AG-R1	0.032 ± 0.006
AG-R2	0.017 ± 0.008
AG-R4	0.027 ± 0.002

Source: Elaborated by the authors.

Regarding a potential application as a dressing, Ma *et al.* (2001) mention that artificial skin substitutes (dressings) are mostly thinner than human dermis, which varies in thickness from 0.5 mm to 2.0 mm, depending on age, sex, and body area. Thus, considering the obtained thicknesses, both films can be used as skin dressings, as seen in the data from **Fig. 2**.

3.2. Water vapor permeability

The data obtained regarding the flow and water vapor permeability of the films are presented in **Fig. 3**. Regarding the total flux (J), the presence of glycerol led to an increase in both films. This process indicates a similar behavior in the films, suggesting that the cross-linking process via short cycles did not interfere with the total flux.

When analyzing the water vapor permeability (Pw), distinctions between the films are observed, such that with the addition of glycerol (AG), there is an increase in Pw. This is because the addition of glycerol makes the polymeric network less dense (as shown by the density data, where the AG film has a lower density when compared to the A film) and consequently more permeable. However, upon initiating the cooling and heating cycles, distinct alterations in Pw are observed, as its density varies according to the number of cycles.

Such data is consistent with the density data (**Fig. 2**), where the AG-R2 film shows densification compared to the others, reducing its permeability rate. This densification allowed for more inter-chain interactions (starch-glycerol) to be established, reducing the water diffusion rate within the film.

Usually, wound dressings are designed with levels of water vapor permeability that allow sufficient exchange of gases and moisture between the wound and the surrounding environment, facilitating optimal healing (Gobi *et al.*, 2021). However, specific permeability values may vary depending on the type and severity of the wound and the individual needs of the patient.

There is no fixed value of water vapor permeability (Pw) specific to wound dressings that promote cellular migration, as the effectiveness of dressings depends on various factors, including the type of wound, the patient's health condition, among others.

Nevertheless, the dressing's ability to exchange water vapor between the wound surface and the surrounding environment is essential to create an ideal healing environment. Thus, the produced films have the potential for practical use in clinical applications, providing crucial support for wound healing as they exhibit water vapor permeability.

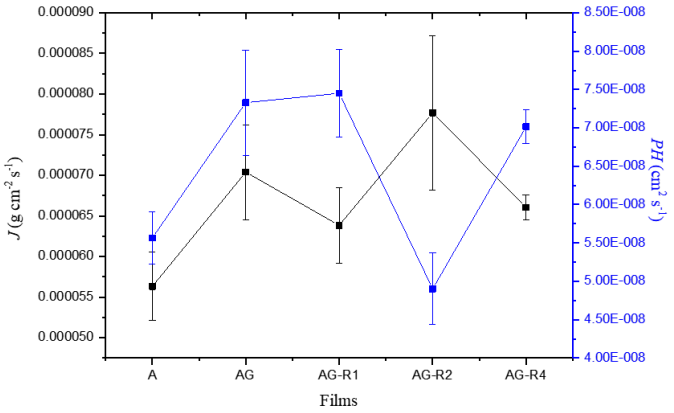

Figure 3. The relationship between the total flux (J) and the water vapor permeability (Pw) of the films.
Source: Elaborated by the authors.

3.3. Scanning electron microscopy (SEM)

Figure 4 presents micrographs of the films' surface and fracture. The micrographs reveal a homogeneous structure in these films; however, some undissolved starch granules are observed, especially in the films with glycerol, which may be related to insufficient agitation time or the temperature used for their preparation.

In the case of film A, the presence of some lines is due to removing the film from the mold, as it strongly adheres to the mold, making its removal more difficult. Regarding the presence of glycerol, it is known to permeate within the polyhydroxylated polymer chain, interrupting inter- and intramolecular interactions, making the polymer plasticized and more flexible (Rodrigues *et al.*, 2021).

Analyzing the micrographs of the films containing glycerol, a homogeneous and dense structure is observed, demonstrating the compatibility between starch and glycerol, as visualized through the cross-section of the film compared to the pure starch film.

The compact and dense morphology remains unchanged with the addition of the cooling and heating step, as observed for the AG-R1 film. The presence of micro-cracks on the surface of the AG-R2 and AG-R4 films, as well as the darkening of the images compared to the other films, is also noted.

The formation of cracks appears to be superficial, not extending into the interior of the films, as seen in the images of the cross-section. The formation of cracks may be due to the number of cycles imposed on these samples, which decreased the solvent present (water) during the film formation process. However, the cracks did not influence the permeation data, especially for the AG-R2 sample.

https://doi.org/10.26850/1678-4618.eq.v51.2026.e1604

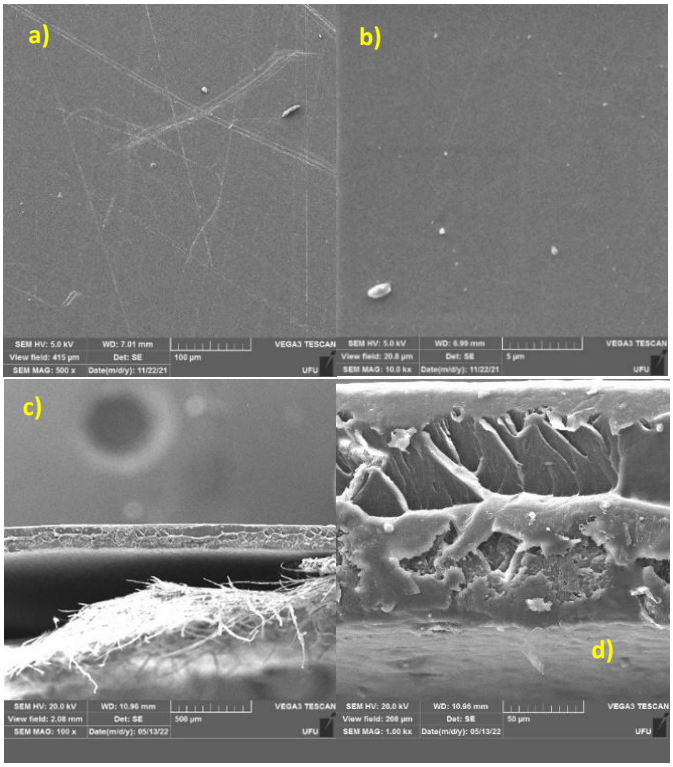

A

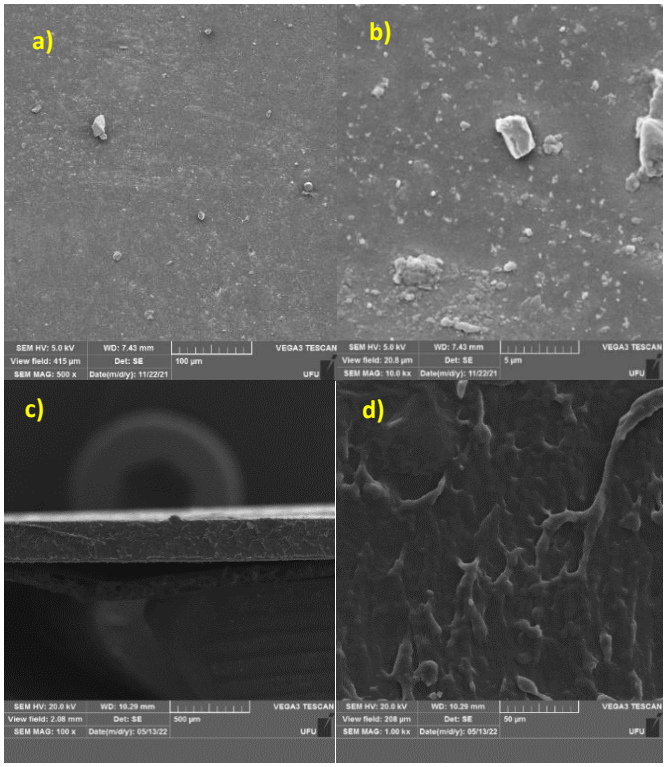

AG-R1

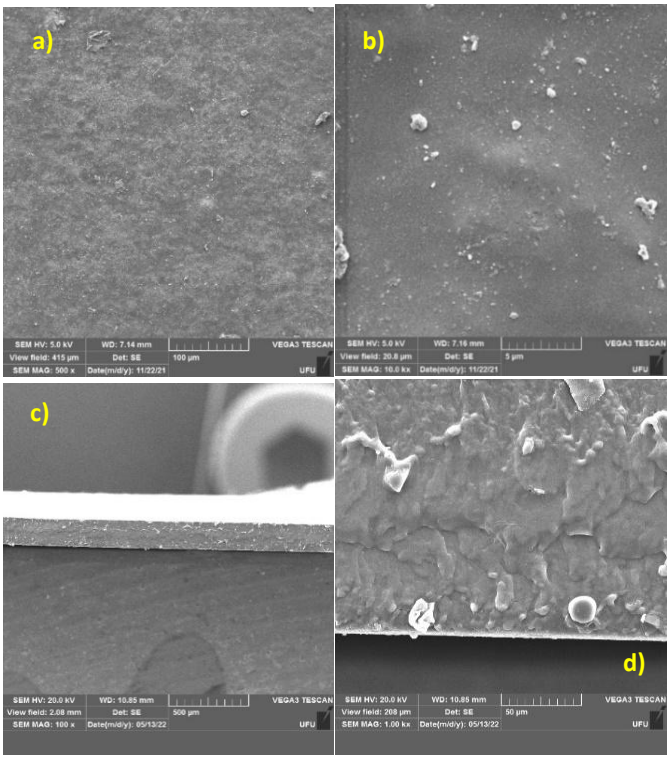

AG

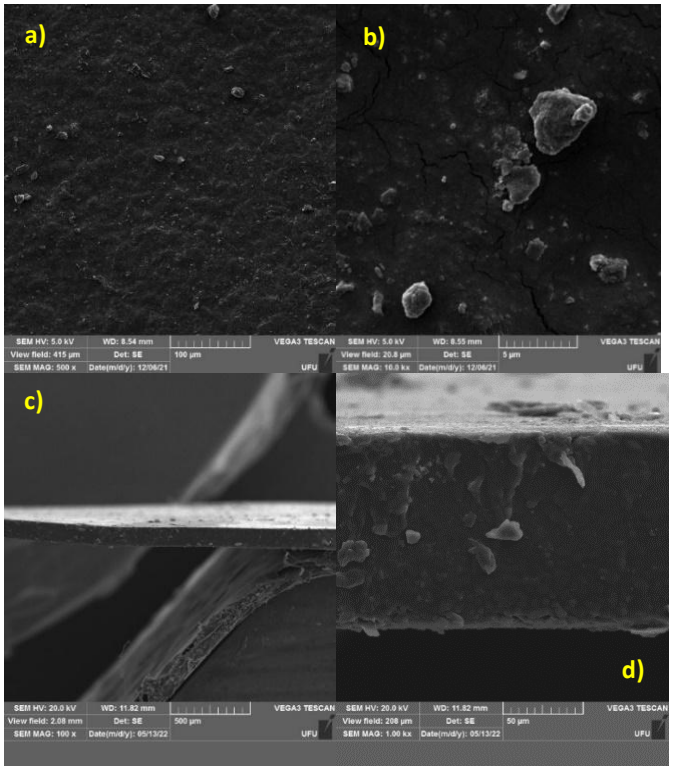

G-R2

https://doi.org/10.26850/1678-4618.eq.v51.2026.e1604

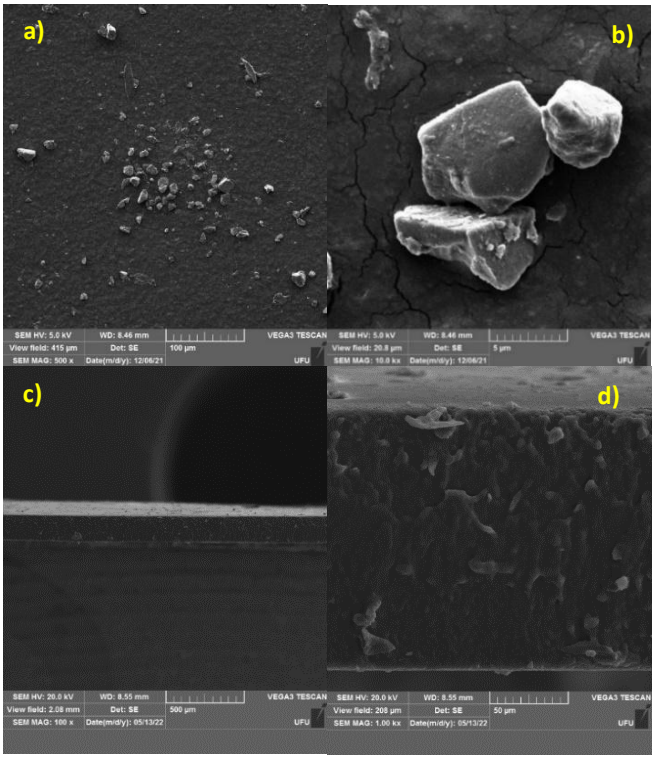

AG-R4

Figure 4. Surface micrographs **A**, **AG**, **AG-R1**, **AG-R2**, **AG-R4**: **(a)** 500x and **(b)** 10.000x magnifications. Film fractures: **(c)** 100x and **(d)** 1.000x magnifications.
Source: Elaborated by the authors.

3.4. X-Ray diffraction

The X-ray diffraction patterns of the produced films, along with the starch in powder form, are presented in **Fig. 5**. Analyzing the diffractograms of the starch granule used in the study, peaks are observed around 15, 17, 18, and 23°, characteristic of type A starch. Regarding the diffractograms of the films, it is noted that for the standard film (Starch), there was a loss in the structural order of the starch, showing a diffractogram of a typically amorphous material. The starch granule, when heated in excess water, undergoes swelling with subsequent rupture and disappearance of the structural order, causing changes or loss in their crystallinity (Van Soest and Vliegenthart, 1997).

Thus, the starch gelatinization process to produce the films resulted in the loss of its long-range structural order. However, with the incorporation of glycerol, the appearance of characteristic peaks in the starch diffraction pattern is observed, indicating an increase in structural order. This structural increase occurred because glycerol interacted through hydrogen bonding with the starch chains, resulting in the rearrangement of the film structure, as observed in the study by Rodrigues *et al.* (2021).

Furthermore, it is observed that this structural rearrangement changes according to the cooling and heating cycles. In this case, the cross-linking process via cooling and heating reduces the intensity of the diffraction peaks compared to the AG film and the formation of three-dimensionally ordered regions. This reduction is due to the reduced mobility of the polymer chains resulting from the cooling process, which increases the viscosity of the polymer solution, thus hindering the rearrangement of the chains.

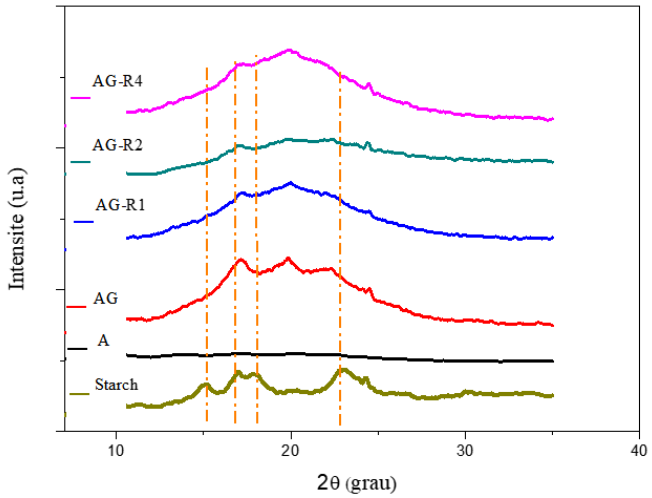

Figure 5. X-ray diffractograms of the films and starch in powder form.
Source: Elaborated by the authors.

3.5. Mechanical properties

The evaluation of the mechanical properties of the films in relation to their tensile strength and deformation capacity was performed to verify the influence of the incorporation of glycerol and to correlate the results obtained with its application. The stress-strain characteristic curves of the films are shown below (**Fig. 6**). The parameters of the ultimate tensile stress, elongation at break and Young's modulus are shown in **Table 2**.

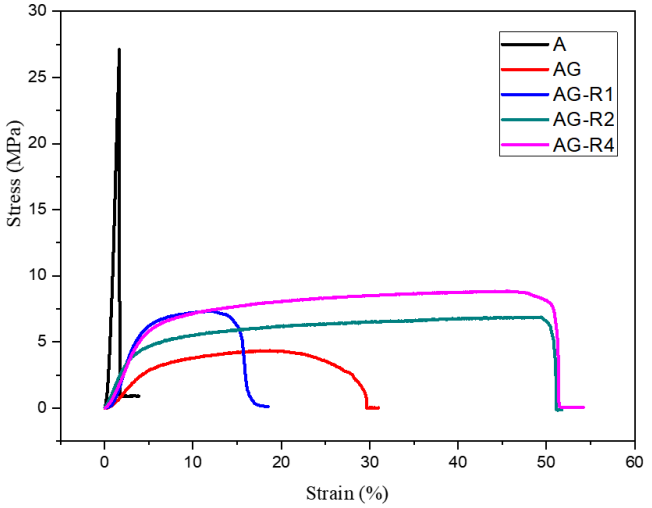

Figure 6. Stress-strain curves of the films tested under controlled atmosphere and temperature.
Source: Elaborated by the authors.

With the incorporation of glycerol into the starch matrix, a change in the mechanical behavior of the films is observed, varying from brittle to ductile. This change is due to the plasticizing nature of glycerol, which reduces the rigidity of the polymeric matrix, as shown by the values of the Young's modulus (E) in **Table 2**, which are drastically reduced by the insertion of glycerol into the starch matrix, thus facilitating the sliding between the starch chains and favoring the deformation of the film during the application of tension.

With the adoption of short cooling and heating cycles, it is observed that they alter both the deformation rate of the cross-

linked films and their tensile strength. Regarding the change in tensile strength, an increase was observed with the execution of the cycles, as the cross-linking process via short cycles of cooling and heating promotes an increase in the intermolecular attractive forces between the components of the polymeric matrix and a reduction in free volume, resulting in a structure with a higher cross-linking density and causing an increase in the stress required for bond rupture.

Table 2. Data related to tensile strength (σrupture), strain at rupture (εrupture), and elastic modulus (E) of the films.

Films	σ rupture (MPa)	ε rupture (%)	E (MPa)
A	26 ± 2	2 ± 1	2,203 ± 3
AG	4 ± 2	30 ± 1	76 ± 2
AG-R1	7 ± 1	19 ± 3	185 ± 1
AG-R2	7 ± 2	51 ± 3	58 ± 2
AG-R4	9±1	53 ± 2	92 ± 2

Source: Elaborated by the authors.

This result is consistent with the study by Millon and Wan (2006), who investigated the influence of the number of freeze-thaw cycles on the mechanical properties of PVA and found that an increase in the number of cycles significantly enhances the tensile strength of their samples. The authors also state that this increase in mechanical properties is due to the formation of structures with a high density of intermolecular contact points, which limit the relative movement between the polymer chains.

Regarding the deformation rate, compared to the AG film, there was a reduction starting from the use of 1 cycle and a subsequent increase with the adoption of 2 and 4 cycles. Similar results were observed by Bornhausen *et al*. (2011) who obtained starch and collagen hydrogels via freeze-thaw cycles and found that an increase in the number of cycles could yield matrices with improved mechanical properties.

The data obtained suggest that even with a reduction in chain mobility resulting from an increase in the attractive intermolecular forces between the constituents of the polymeric matrix, glycerol still effectively acts as a plasticizing agent, causing sliding between the starch chains and thus favoring the deformation of the film during the application of tension.

3.6. Swelling and solubility studies at physiological pH

The data concerning the swelling capacity of the films are presented in **Fig. 7**. Analyzing the graph, it is observed that both films exhibit high swelling rates, which change with the introduction of glycerol and the adoption of the heating and cooling cycles. In the initial times, the swelling of films increased significantly due to the free volume in their structure. However, this increase is reduced by cross-linking, which causes the solvent to encounter the cross-linking points, which act as obstacles for the diffusing solvent, thus maintaining the swelling rate almost constant (Peppas, 2010).

Analyzing each film, it was found that the A and AG-R4 films disintegrated when handled after 30 min of immersion in PBS, thus preventing their complete analysis. The other films, AG, AG-R1, and AG-R2, presented similar swelling profiles, with slight modifications regarding the AG-R1 film, which reached the equilibrium state after 2 h of immersion, while the AG and AG-R2 films reached equilibrium after 30 min of immersion. The time it takes for the hydrogel to reach equilibrium is related to the cross-linking density present in the structure, as an increase in cross-linking density results in an increase in resistive force, causing the hydrogels to reach an equilibrium state in a shorter time (Kirschner and Anseth, 2013).

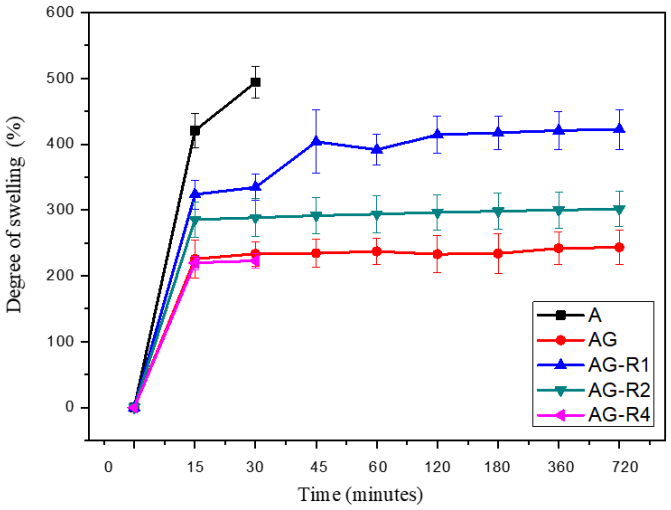

Figure 7. Degree of swelling of films.
Source: Elaborated by the authors.

As glycerol forms hydrogen bonds with starch, breaking the current hydrogen bonds between the hydroxyl groups in the starch molecules, this leads to the formation of new hydrogen bonds between the glycerol and hydroxyl groups of the starch. As a result, cross-linking points are formed, meaning structures with a higher density of intermolecular contact points, as seen in the mechanical test data, making it more difficult for water molecules to penetrate the films. This explains the reduction in the degree of swelling in the AG film compared to the films cross-linked through cycles.

It is thus observed that, compared to AG, with the incorporation of the cooling and heating cycles, the degree of swelling increases, but at a rate lower than that of the A film. This increase occurs because even though glycerol forms new hydrogen bonds between the hydroxyl groups of the starch, the cooling process promotes an increase in the intermolecular attractive forces between the components of the polymeric matrix and a consequent reduction in free volume, resulting in a structure with a higher cross-linking density, thus increasing the degree of cross-linking.

It is also noted that this increase is reduced with an increase in the number of cycles (AG-R1>AG-R2>AG-R4), as observed in the study by Hassan and Peppas (2000), who prepared PVA hydrogels through freeze-thaw cycles and found that the samples subjected to fewer cycles exhibited a higher degree of swelling.

An increase in the number of cycles leads to a reduction in chain movement, which reduces the films' apparent crystallinity. This is observed in **Fig. 5**, where the films obtained with cooling and heating cycles exhibited lower peak intensities in the diffraction patterns than the glycerol film (AG) and a more amorphous character. Since the cycles are performed over short periods, the chains do not have enough time to reorganize effectively, resulting in a lower degree of apparent crystallinity.

Thus, although the increase in the number of cycles did not result in an ordered structure, it was favorable for the formation of a three-dimensional network with less free volume, which hinders solvent penetration, as the cycles contribute to the entanglement of the chains, as observed in the study by Millon and Wan (2006).

However, this procedure reaches a limit, which explains the behavior of the AG-R4 sample that did not remain intact (disintegrated after 30 min of immersion), indicating that its cross-linking can be easily reversed when in physiological conditions, such as immersion in PBS. Regarding the solubility of the films

(Table 3), it can be observed that during the analysis period, i.e., 48 h, the solubility rate of the films underwent modifications. The film completely dissolves due to the high hydrophilicity of the starch, justified by the fact that starch is a highly hygroscopic polysaccharide, disintegrating rapidly into an aqueous medium.

The incorporation of glycerol into the films results in a reduction in solubility, except for the AG-R4 film. This reduction results from the cross-linking process that promotes effective interaction between glycerol and starch chains, thereby reducing its ability to interact with the solvent molecules, as shown by the swelling results. This reduction in solubility is greater in films subjected to cooling and heating cycles, as in this case, cross-linking occurs more effectively, resulting in denser films, as indicated by the thickness and density data.

Table 3. Solubility values of the films after 48 h in PBS.

Films	Solubility (%)
A	100.0 ± 0.0
AG	12.7 ± 0.7
AG-R1	9.0 ± 0.5
AG-R2	7.5 ± 0.5
AG-R4	96.0 ± 0.8

Source: Elaborated by the authors.

It should be noted that the AG-R4 film showed high solubility, indicating that cross-linking was not effective in this sample, and the entanglement formed is easily reversible, as verified in the swelling results. Thus, the presence of glycerol alone can favor the cross-linking of the films; however, the presence of the heating and cooling cycles modifies this process, favoring the strengthening of the interaction of glycerol molecules with the starch chains, thereby restricting the entry of solvent into the film structure and reducing its solubility, as shown by the results obtained for the AG-R1 and AG-R2 films.

A less soluble material can be used as a dermal dressing; therefore, the decrease in the solubility of the films in PBS, which simulates physiological pH, is a positive factor for their application as a biomaterial. Thus, considering a potential application of the films as a dressing, the method adopted to produce AG-R2 resulted in a more cross-linked film due to the lower volume, which resulted in higher density and low solubility. Furthermore, despite the reduction in solubility, the AG-R2 film still exhibits a high swelling rate, which is expected for hydrogels. This swelling capacity indicates that it effectively absorbs exudates released from wounds without disintegrating during its use.

4. Conclusions

In the present study, the effectiveness of the physical cross-linking process of starch hydrogels was investigated via short cycles of cooling and heating in the presence of glycerol. The results obtained show that the incorporation of 30% glycerol promoted the cross-linking of the films, which was altered by the cooling and heating process. In this case, the cycles favored cross-linking density, promoting the densification of the films due to the approximation of the polymeric chains through the formation of hydrogen bonds between the starch chains and the glycerol molecules. However, considering that the physical cross-linking process is reversible, it can be observed that the adoption of 2 cycles resulted in a more stable cross-linking, as the AG-R2 film showed a significant reduction in volume (lower thickness) compared to the other films.

Regarding the results at physiological pH, it was found that the films produced via cycles of cooling and heating exhibit swelling capacity that favors their use as dermal dressings; however, the AG-R1 and AG-R2 films appear to be more suitable. Compared to these two samples, the process used in the AG-R2 sample resulted in a film with less free volume, indicating that the mentioned process is more effective in promoting the formation of cross-links between the starch chains and the glycerol molecules, which was confirmed through the results of water vapor permeation, swelling, and solubility. It responded better in terms of mechanical properties.

For future studies, conducting a more in-depth investigation of the biological properties and biocompatibility of cross-linked starch hydrogel films, especially regarding their interaction with biological tissues, immune response, and wound healing processes, is recommended. Furthermore, it would be interesting to explore the influence of different concentrations of glycerol and parameters of cooling and heating cycles on the structure and properties of the films, to further optimize their stability, strength, and exudate absorption capacity. Investigations into the degradation of the films in physiological environments and studies on the controlled release of therapeutic compounds would also be valuable in expanding the potential applications of these materials as biomedical dressings.

Authors' contribution

Conceptualization: Mariana Fornaizer; Harumi Otaguro; **Data curation**: Mariana Fornaizer; Harumi Otaguro; **Formal Analysis**: Mariana Fornaizer; Harumi Otaguro; **Funding acquisition**: Not applicable; **Investigation**: Mariana Fornaizer; **Methodology**: Mariana Fornaizer; **Project administration**: Mariana Fornaizer; Harumi Otaguro; **Resources**: Not applicable; **Software**: Mariana Fornaizer; **Supervision**: Harumi Otaguro; **Validation**: Mariana Fornaizer; Harumi Otaguro; **Visualization**: Mariana Fornaizer; **Writing – original draft**: Mariana Fornaizer; **Writing – review & editing**: Mariana Fornaizer; Harumi Otaguro.

Conflict of interest

The authors declare that there is no conflict of interest.

Data availability statement

All data sets were generated or analyzed in the current study.

Artificial Intelligence usage statement

The authors declare that they did not use Artificial Intelligence tools at any stage of the preparation, correction, or evaluation of this work.

Funding

Not applicable.

Acknowledgments

Not applicable.

References

Abdullah, T.; Su, E.; Memić, A. Designing Silk-Based Cryogels for Biomedical Applications. *Biomimetics.* **2022**, *8* (1), 5. https://doi.org/10.3390/biomimetics8010005

Bai, H.; Zhang, Z.; Huo, Y.; Shen, Y.; Qin, M.; Feng, W. Tetradic Double-Network Physical Crosslinking Hydrogels with Synergistic High Stretchable, Self-Healing, Adhesive, and Strain-Sensitive Properties. *J.*

Mater. Sci. Technol. **2022**, *98*, 169–176. https://doi.org/10.1016/j.jmst.2021.05.020

Ben, Z. Y.; Samsudin, H.; Yhaya, M. F. Glycerol: Its Properties, Polymer Synthesis, and Applications in Starch-Based Films. *Eur. Polym. J.* **2022**, *175*, 111377. https://doi.org/10.1016/j.eurpolymj.2022.111377

Bornhausen, K.; Silva, J. F.; Domiciano, M. G.; Gon, R. L. R.; Valderrama, P.; Silva, R. Síntese de Hidrogéis de Amido e Colágeno Através de Ciclos de Congelamento e Descongelamento. In: Anais da 34ª Reunião Anual da Sociedade Brasileira de Química 2011.

Costa, D. D.; Santos, A. D.; Silva, E. D.; Silva, I. D. Desenvolvimento e Caracterização de Filmes à Base de Amido de Feijão Macáçar (*Vigna unguiculata* (L.) Wap). *Holos.* **2017**, *7*, 2–16. https://doi.org/10.15628/holos.2017.6318

Dong, X.; Yao, F.; Jiang, L.; Liang, L.; Sun, H.; He, S.; Li, J. Facile Preparation of a Thermosensitive and Antibiofouling Physically Crosslinked Hydrogel/Powder for Wound Healing. *J. Mater. Chem. B.* **2022**, *10* (13), 2215–2229. https://doi.org/10.1039/D2TB00027J

Fan, C.; Xu, Q.; Hao, R.; Wang, C.; Que, Y.; Chen, Y.; Chang, J. Multi-Functional Wound Dressings Based on Silicate Bioactive Materials. *Biomaterials.* **2022**, *287*, 121652. https://doi.org/10.1016/j.biomaterials.2022.121652

Fornazier, M.; Gontijo de Melo, P.; Pasquini, D.; Otaguro, H.; Pompêu, G. C. S.; Ruggiero, R. Additives Incorporated in Cellulose Acetate Membranes to Improve Its Performance as a Barrier in Periodontal Treatment. *Front. Dent. Med.* **2021**, *2*, 776887. https://doi.org/10.3389/fdmed.2021.776887

Gobi, R.; Ravichandiran, P.; Babu, R. S.; Yoo, D. J. Biopolymer and Synthetic Polymer-Based Nanocomposites in Wound Dressing Applications: A Review. *Polymers.* **2021**, *13* (12), 1962. https://doi.org/10.3390/polym13121962

Gerrits, L.; Bakker, B.; Hendriks, L. D.; Engels, S.; Hammink, R.; Kouwer, P. H. Tailoring of Physical Properties in Macroporous Poly (Isocyanopeptide) Cryogels. *Biomacromolecules.* **2024**, *25* (6), 3464–3474. https://doi.org/10.1021/acs.biomac.4c00086

Guo, Y.; Wu, M.; Li, R.; Cai, Z.; Zhang, H. Thermostable Physically Crosslinked Cryogel from Carboxymethylated Konjac Glucomannan Fabricated by Freeze-Thawing. *Food Hydrocoll.* **2022**, *122*, 107103. https://doi.org/10.1016/j.foodhyd.2021.107103

Hassan, C. M.; Peppas, N. A. Structure and Applications of Poly(vinyl alcohol) Hydrogels Produced by Conventional Crosslinking or by Freezing/Thawing Methods. In *Biopolymers: PVA Hydrogels, Anionic Polymerisation, Nanocomposites*; *Advances in Polymer Science*, Vol. 153; Springer: Berlin, Heidelberg, 2000; pp 37–65; https://doi.org/10.1007/3-540-46414-X_2

He, Z.; Woo, M. W.; Shan, Z.; Dai, R.; Cheng, F.; Chen, H. Preparation and Characterization of Crosslinked Starch Films Pretreated with Sodium Hydroxide/Amide/Water Solvent System. Colloids and Surfaces A: Physicochemical and Engineering Aspects 2022, 650, 129544. https://doi.org/10.1016/j.colsurfa.2022.129544

Jia, Y.; Hsu, Y. I.; Uyama, H. A Starch-Based, Crosslinked Blend Film with Seawater-Specific Dissolution Characteristics. *Carbohydr. Polym.* **2023**, *299*, 120181. https://doi.org/10.1016/j.carbpol.2022.120181

Kirschner, C. M.; Anseth, K. S. Hydrogels in Healthcare: From Static to Dynamic Material Microenvironments. *Acta Mater.* **2013**, *61* (3), 931–944. https://doi.org/10.1016/j.actamat.2012.10.037

Long, L.; Liu, W.; Hu, C.; Yang, L.; Wang, Y. Construction of Multifunctional Wound Dressings with Their Application in Chronic Wound Treatment. *Biomater. Sci.* **2022**, *10* (15), 4058–4076. https://doi.org/10.1039/D2BM00620K

Lu, L.; Huang, Z.; Li, X.; Li, X.; Cui, B.; Yuan, C.; Dai, Q. A High-Conductive, Anti-Freezing, Antibacterial and Anti-Swelling Starch-Based Physical Hydrogel for Multifunctional Flexible Wearable Sensors. *Int. J. Biol. Macromol.* **2022**, *213*, 791–803. https://doi.org/10.1016/j.ijbiomac.2022.06.011

Ma, J.; Wang, H.; He, B.; Chen, J. A Preliminary In Vitro Study on the Fabrication and Tissue Engineering Applications of a Novel Chitosan Bilayer Material as a Scaffold of Human Neofetal Dermal Fibroblasts. *Biomaterials.* **2001**, *22* (4), 331–336. https://doi.org/10.1016/S0142-9612(00)00188-5

Mantha, S.; Pillai, S.; Khayambashi, P.; Upadhyay, A.; Zhang, Y.; Tao, O.; Tran, S. D. Smart Hydrogels in Tissue Engineering and Regenerative Medicine. *Materials.* **2019**, *12* (20), 3323. https://doi.org/10.3390/ma12203323

Matta Jr, M. D. D.; Sarmento, S.; Sarantópoulos, C. I.; Zocchi, S. S. Propriedades de Barreira e Solubilidade de Filmes de Amido de Ervilha Associado com Goma Xantana e Glicerol. *Polímeros.* **2011**, *21*, 67–72. https://doi.org/10.1590/S0104-14282011005000011

Millon, L. E.; Wan, W. K. The Polyvinyl Alcohol–Bacterial Cellulose System as a New Nanocomposite for Biomedical Applications. *J. Biomed. Mater. Res. B Appl. Biomater.* **2006**, *79* (2), 245–253. https://doi.org/10.1002/jbm.b.30535

Palanisamy, C. P.; Cui, B.; Zhang, H.; Gunasekaran, V. P.; Ariyo, A. L.; Jayaraman, S.; Long, Q. A Critical Review on Starch-Based Electrospun Nanofibrous Scaffolds for Wound Healing Application. *Int. J. Biol. Macromol.* **2022**, *222*, 1852–1860. https://doi.org/10.1016/j.ijbiomac.2022.09.274

Peppas, N. A. *Biomedical Applications of Hydrogels Handbook*. Springer Science & Business Media, 2010.

Pires, V. G.; Moura, M. R. D. Preparação de Novos Filmes Poliméricos Contendo Nanoemulsões do Óleo de Melaleuca, Copaíba e Limão para Aplicação como Biomaterial. *Quím. Nova.* **2017**, *40*, 1–5. https://doi.org/10.21577/0100-4042.20160130

Rodrigues, S.; Fornazier, M.; Magalhães, D.; Ruggiero, R. Potential Utilization of Glycerol as Crosslinker in Starch Films for Application in Regenerative Dentistry. *Res. Soc. Dev.* **2021**, *10* (16), e148101623640. https://doi.org/10.33448/rsd-v10i16.23640

Savencu, I.; Iurian, S.; Porfire, A.; Bogdan, C.; Tomuță, I. Review of Advances in Polymeric Wound Dressing Films. *React. Funct. Polym.* **2021**, *168*, 105059. https://doi.org/10.1016/j.reactfunctpolym.2021.105059

Souza, L. D.; Vieira, P. R.; Florindo, R. H. D. S.; Alavarse, A. C.; Bonvent, J. J. Features and Strategies for Scaffold Design and Production for Tissue Engineering. *Quím. Nova.* **2022**, *45*, 816–830. https://doi.org/10.21577/0100-4042.20170876

Van Soest, J. J.; Vliegenthart, J. F. Crystallinity in Starch Plastics: Consequences for Material Properties. *Trends Biotechnol.* **1997**, *15* (6), 208–213. https://doi.org/10.1016/S0167-7799(97)01021-4

Wang, B.; Yu, B.; Yuan, C.; Guo, L.; Liu, P.; Gao, W.; Abd El-Aty, A. M. An Overview on Plasticized Biodegradable Corn Starch-Based Films: The Physicochemical Properties and Gelatinization Process. *Crit. Rev. Food Sci. Nutr.* **2022**, *62* (10), 2569–2579. https://doi.org/10.1080/10408398.2020.1868971

Xiang, Y.; Xian, S.; Ollier, R. C.; Yu, S.; Su, B.; Pramudya, I.; Webber, M. J. Diboronate Crosslinking: Introducing Glucose Specificity in Glucose-Responsive Dynamic-Covalent Networks. Journal of Controlled Release 2022, 348, 601–611. https://doi.org/10.1016/j.jconrel.2022.06.016

Yan, K.; Wan, Y.; Xu, F.; Lu, J.; Yang, C.; Li, X.; Wang, D. Ionic Crosslinking of Alginate/Carboxymethyl Chitosan Fluorescent Hydrogel for Bacterial Detection and Sterilization. *Carbohydr. Polym.* **2023**, *302*, 120427. https://doi.org/10.1016/j.carbpol.2022.120427

Zeng, Z.; Zhu, M.; Chen, L.; Zhang, Y.; Lu, T.; Deng, Y.; Xiong, R. Design the Molecule Structures to Achieve Functional Advantages of Hydrogel Wound Dressings: Advances and Strategies. *Compos. Part B Eng.* **2022**, 110313. https://doi.org/10.1016/j.compositesb.2022.110313